nature protocols

https://doi.org/10.1038/s41596-025-01192-2

Protocol

Check for updates

Highly stable planar asymmetric suspended membranes for investigating protein dynamics and membrane fusion

Manindra Bera[1,2], Ramalingam Venkat Kalyana Sundaram[1,2], Jeff Coleman[1,2], Atrouli Chatterjee[1,2], Sikha Thoduvayil[1,3], Frederic Pincet[1,4] ✉ & Sathish Ramakrishnan[1,3] ✉

Abstract

Membrane fusion is central to cellular signaling and trafficking, requiring a detailed understanding of protein–lipid interactions. Studying these dynamic events in live cells presents challenges due to their complexity and heterogeneity. To address this, we developed a reductionist in vitro membrane model system that enables the controlled investigation of individual molecular components. This approach begins with a minimal membrane environment, with the opportunity for the stepwise addition of specific components to incrementally increase complexity achieving a level of experimental precision often unattainable in cellular studies. We developed suspended lipid membranes, a platform that uses pore-spanning lipid bilayers formed on microfabricated silicon chips with micrometer-sized holes. These membranes closely mimic native cellular architecture by maintaining aqueous compartments on both sides, providing a solvent-free, near-native environment with exceptional lateral diffusion properties. Their high stability makes them ideal for time-lapse imaging and dynamic process analysis using total internal reflection fluorescence and confocal microscopy. Here we present a detailed protocol for generating pore-spanning, planar suspended lipid membranes from native and synthetic reconstituted lipids using our silicon chip platform. Using SNARE proteins and molecular chaperones, we demonstrate the system's ability to capture ultrafast membrane fusion events. Additionally, we demonstrate single-molecule protein counting, protein dynamics analysis and single-vesicle fusion assays using fluorescently labeled proteins and vesicles. The ability to preserve native lipid asymmetry, biological composition and lateral diffusion makes this method a powerful tool for dissecting membrane fusion mechanisms and other membrane biological processes with unparalleled precision.

Key points

- Membrane fusion is a complex biological process important in signal transduction. This protocol can be used to create, for example, a neuronal synapse on a chip that contains a readily releasable pool of vesicles triggered by calcium.
- The experiment is performed on a chip where an asymmetric membrane is suspended across micrometer-sized holes, allowing fluorophore-labeled proteins and lipids to be visualized using total internal reflection and confocal microscopy.

Key references

Kalyana Sundaram, R. V. et al. *Small* **18**, 2205567 (2022): https://doi.org/10.1002/smll.202205567

Ramakrishnan, S. et al. *Langmuir* **34**, 5849–5859 (2018): https://doi.org/10.1021/acs.langmuir.8b00116

Ramakrishnan, S. et al. *eLife* **9**, e54506 (2020): https://doi.org/10.7554/eLife.54506

Kalyana Sundaram, R. V. et al. PNAS (2023): https://doi.org/10.1073/pnas.2309516120

Bera, M et al. *Proc. Natl Acad. Sci.* **120**, e2311484120 (2023): https://doi.org/10.1073/pnas.2311484120

[1]Yale Nanobiology Institute, West Haven, CT, USA. [2]Department of Cell Biology, Yale University School of Medicine, New Haven, CT, USA. [3]Department of Pathology, Yale University School of Medicine, New Haven, CT, USA. [4]Laboratoire de Physique de l'Ecole Normale Superieure, Ecole Normale Superieure (ENS), Universite Paris Sciences et Lettres (PSL), CNRS, Sorbonne Universite, Universite Paris-Cite, Paris, France. ✉e-mail: frederic.pincet@yale.edu; sathish.ramakrishnan@yale.edu

Introduction

Eukaryotes use SNARE protein-mediated fusion to release chemicals, peptides and hormones to regulate growth, communication and metabolism[1–5]. Depending on the physiology, precise constraints over vesicle size and rate of exocytosis control the flow of substance and information to maintain metabolic homeostasis. For example, at neuronal synapses, the first synaptic vesicles can release neurotransmitters in 0.2–1 ms after action potential stimulation to keep up the pace of neural circuitry[6]. Despite extensive study, vesicle fusion remains only partially understood owing to the complex and intricate biochemical composition of synapses; more than 250 proteins have been identified, yet only a fraction of them have been characterized in detail[7,8]. To elucidate the functions of these proteins and their specific roles in vesicle fusion in vivo presents substantial challenges. The dense molecular environment and the numerous interacting proteins in neurons make it difficult to isolate individual protein functions. The knowledge we could gain from in vivo studies is sometimes clouded by the complexity of the cell, and may require fixation[9] or gel-expansion of the samples[10]. To circumvent these challenges, cell-free systems have been developed to allow examination of key components in a more controlled setting. Small unilamellar vesicles (SUVs) or liposomes, supported lipid bilayers (SLBs) and giant unilamellar vesicles (GUVs) have become popular models for studying exocytosis owing to their ability to mimic the minimal machinery needed for membrane fusion. This allows the individual labeling of proteins using maleimide-thiol or NHS ester-amine chemistry to study the behavior of the proteins in situ.

While efficient, the reductionist approach faces challenges, especially in oversimplified models that fail to mimic physiological conditions accurately. An example is the early minimal reconstructions of Ca^{2+}-triggered synaptic vesicle fusion, which utilized liposome–liposome fusion[11–18] or GUV–SUV fusion[19,20]. However, this method fails to replicate the intricate planar-curved architecture characteristic of cellular systems. To overcome these challenges, advanced systems, including SLBs[21,22] and polyethylene glycol-based SLB platforms[23], have been developed to more accurately mimic planar cellular membranes. However, SLBs also face drawbacks. Notably, the proximity of the bilayer to the supporting substrate limits the ability of the system to accommodate large, multipass transmembrane proteins with extensive cytoplasmic domains. The small space between the bilayer and the solid support, typically less than a few nanometers, restricts the mobility of proteins with even short cytoplasmic tails. This constraint interferes with the natural dynamics of membrane proteins, impacting their functionality and limiting the utility of SLBs for studying proteins with extended intracellular regions.

Recently, Edwin Chapman's group demonstrated the usage of black lipid membranes (BLMs) and nanodiscs to study SNARE-mediated membrane fusion[24], which offers high temporal resolution and freedom from substrate attachment. It provides lateral lipid and protein diffusion, allowing for real-time analysis of membrane fusion events. However, despite these advantages, potential limitations persist, including the presence of solvent in the membrane, the curved geometry of vesicles and challenges in quantifying processes such as vesicle docking, undocking, priming and fusion kinetics.

Developing membrane models that closely replicate the native environment without organic solvents and allow for exploring biological processes on both sides of the membrane is crucial for dissecting biological mechanisms. The ultimate goal is to create an in vitro platform that offers precise control over each component with nanometric accuracy, high spatial and temporal resolution, lipid asymmetry and the capacity to handle large, multipass membrane proteins and controlled protein copy numbers. Such a platform would provide unparalleled insights into the roles of proteins and lipids in synaptic vesicle exocytosis.

Development of the protocol

Choice of Si/SiO_2 surface

We developed an optimized platform for lipid bilayer formation using silicon (Si) with a silicon dioxide (SiO_2) surface, leveraging its hydrophilicity, chemical versatility and

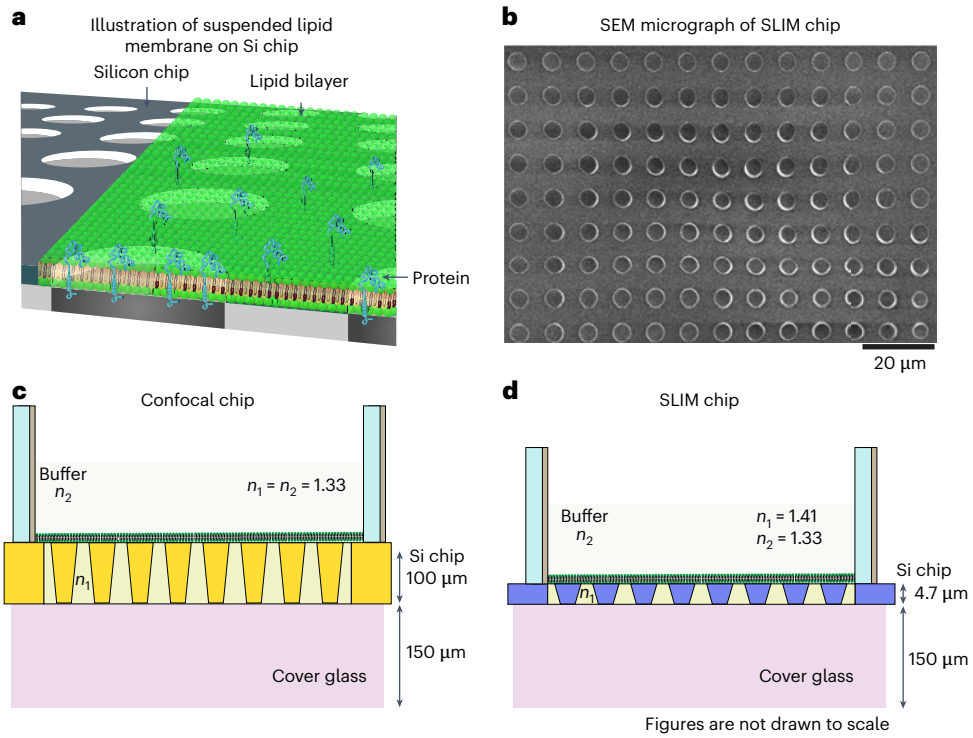

Fig. 1 | The design of the SLIM chips. a, A schematic representation of the suspended bilayer on a Si chip. The Si chip consists of an array of holes that support the lipid bilayer, creating a suspended membrane across the holes. Lipids (green) and proteins (blue ribbon) are mobile in this suspended membrane. **b**, Scanning electron microscope (SEM) image of the SLIM chip, showing an array of 5 µm diameter holes. Scale bar, 20 µm. **c**, A schematic of the confocal chip. The chip features a 150-µm-thick glass support at the bottom and a thick silicon layer of >10 µm (yellow). The lipid bilayer forms on the silicon surface, separating two compartments below and above the bilayer, both maintaining the same buffer solution with a refractive index of 1.33 ($n_1 = n_2$). **d**, A schematic of the SLIM chip, optimized for single-molecule imaging in TIRF microscopy. The bottom support is a 150-µm-thick glass layer, with a silicon layer ranging from 2 to 6 µm in thickness (blue). This design ensures that light illumination focuses solely on the lipid bilayer, enabling high-resolution single-molecule imaging. The design is further optimized for a silicon height of 4.7 µm due to the easy manufacturing of thin silicon wafers. OptiPrep ($n_1 = 1.41$) is used in the silicon wells between the bilayer and cover glass, while the experimental buffer above the bilayer has a refractive index of 1.33 (n_2).

structural stability. The SiO_2 layer promotes efficient lipid spreading and uniform bilayer formation due to its intrinsic hydrophilic nature, which can be further enhanced through plasma treatments to improve bilayer adhesion and longevity. The silicon substrate provides mechanical rigidity, allowing for precise microfabrication of micrometer-sized pores, which support suspended lipid membranes (SLIMs) while maintaining aqueous compartments on both sides, mimicking native cell membranes. This configuration ensures exceptional lateral diffusion for proteins within the suspended region and lipids all over the chip. The Si/SiO_2 interface also enhances experimental reproducibility by enabling surface charge control, which can be further optimized using p-type or n-type silicon, depending on the lipid composition. P-type Si promotes bilayer formation for negatively charged lipids, such as phosphatidylserine or phosphoinositides, whereas n-type Si enhances the stability of positively charged or zwitterionic lipid bilayers, such as 1,2-dioleoyl-3-trimethylammonium propane. This tunability allows for optimized membrane formation across diverse lipid compositions, broadening the platform's applicability for various biological studies.

SLIM as an advanced model system

SLIMs, spanned across micrometer-sized holes in a silicon chip (Fig. 1), overcome the limitations of other lipid models, such as liposomes, droplet lipid bilayers, BLMs and SLBs, by providing

a controlled environment for investigating recalcitrant membrane proteins containing multipass transmembrane domains or members of a higher-order oligomeric complex. Unlike these earlier models, SLIM platforms can closely reproduce the physiological conditions of exocytosis in vitro[25–33]. Building on the established SLIM framework[30], we have developed an advanced version of the SLIM platform, tailored to enable single-molecule imaging and the formation of planar membranes using cell-derived giant plasma membranes. This innovation paves the way for studying membrane fusion under conditions resembling the natural cellular environment. It also facilitates the examination of complex membrane proteins, such as G-protein-coupled receptors, ion channels and receptors, without needing to fix and permeabilize cell membranes[34]. This advancement significantly deepens our understanding of membrane protein function and paves the way for studying various other membrane-related processes on a new platform.

Protocol overview

In this protocol, we provide a straightforward and efficient method for constructing planar SLIMs by inducing the rupture of synthetic (reconstituted) or native GUVs. The buffer composition on both sides of the membrane can be adjusted to meet specific experimental requirements, provided that osmolarity is carefully matched to prevent bilayer rupture. This procedure ensures the structural integrity and functionality of the membranes, which is critical for subsequent studies of vesicle docking and fusion events. The protocol also includes detailed guidelines to process and analyze the resulting data. This comprehensive guide provides detailed instructions for generating synthetic and native GUVs with intact membrane proteins, facilitating their study under a microscope in a planar configuration. Crucially, this protocol allows researchers to prepare lipid membranes with specific membrane proteins of interest, supporting the investigation of their transient interactions and dynamics in single-molecule fluorescence settings (Fig. 2).

Applications and target audience

The protocol described here offers a versatile system for recreating a neuronal synapse on a chip containing a readily releasable pool of vesicles triggered by calcium. This approach allows researchers to study key processes underlying vesicle docking, undocking, and fusion, which are critical for understanding the regulation of neurotransmitter release. The system also enables the study of spontaneous fusion, that is, vesicle fusion that occurs without an external stimulus such as calcium influx, providing insights into basal synaptic activity and its role in maintaining synaptic plasticity. With high temporal and spatial resolution, this method allows researchers to dissect these stages in the vesicle lifecycle, revealing how individual proteins control distinct phases of the fusion process.

Beyond its applications in neuroscience, the protocol is designed to facilitate the reconstitution of any membrane protein into a free-standing planar lipid bilayer, enabling the exploration of various biological processes. In addition to studying vesicle fusion, the system supports investigations into protein–protein interactions, lipid dynamics and the influence of membrane curvature on fusion events. By incorporating proteins into a well-defined bilayer, researchers can examine the specific roles of proteins in membrane remodeling, ligand binding and signal transduction. The system also applies to studying fusion in other contexts, such as hormone secretion and immune cell degranulation. Its flexibility makes it valuable for researchers in membrane biophysics, immunology and cell signaling, providing a platform to study complex membrane processes in near-physiological conditions and offering new opportunities to explore membrane protein dynamics and its interactions at the single-molecule level.

Comparison with alternative methods and advantages

When comparing various membrane models used for studying exocytosis, the planar membrane geometry is particularly advantageous owing to its close resemblance to the cellular plasma membrane. The most commonly used system, SLBs, is effective in mimicking the planar architecture and is well-suited for single molecule imaging techniques, providing

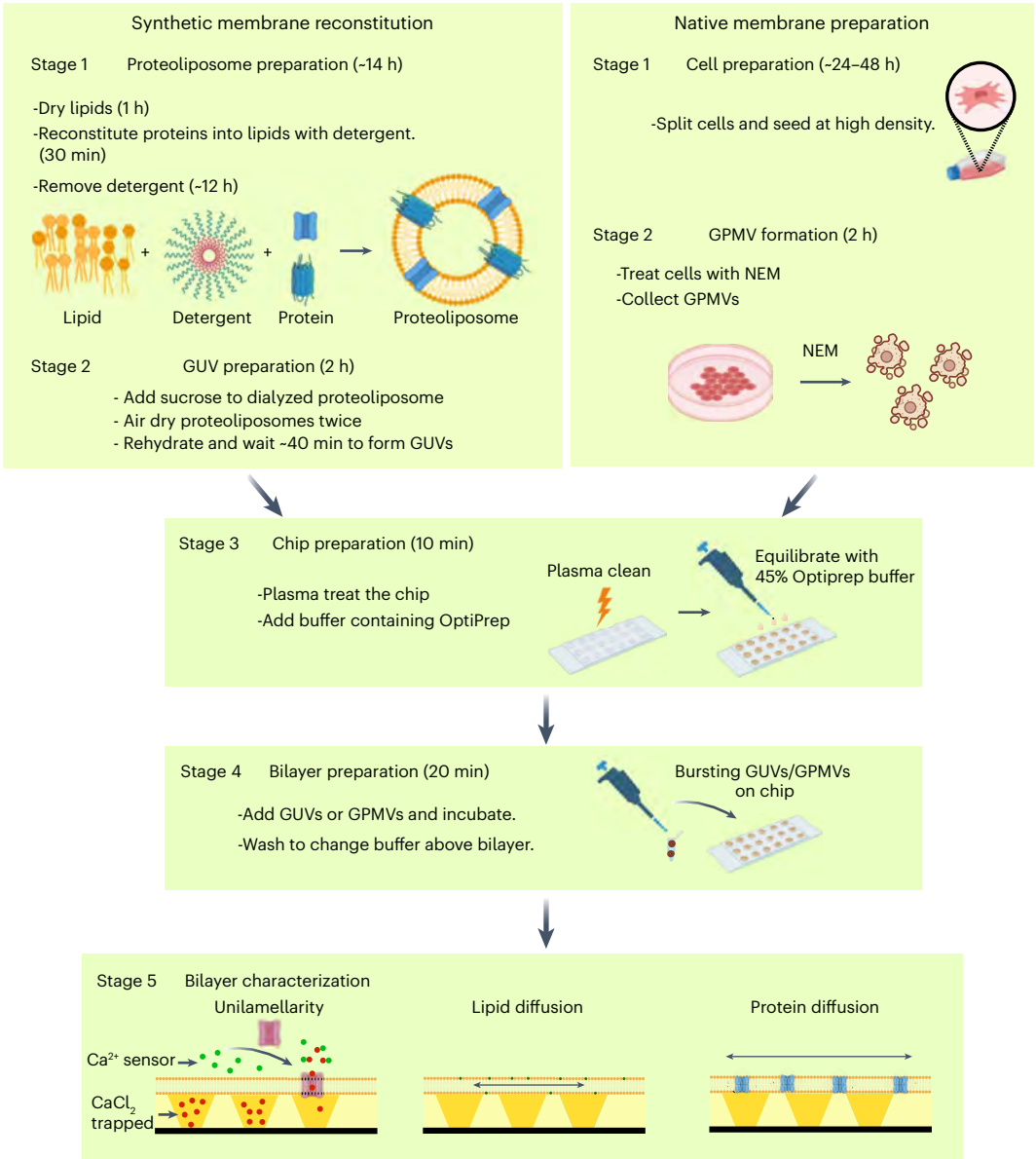

Fig. 2 | A schematic representation of the protocol for reconstituting suspended bilayers using synthetic and native membranes. The diagram outlines the sequential steps involved in bilayer reconstitution. On the left, the preparation of synthetic membranes (proteo-GUVs) is shown, with steps such as drying lipids, reconstituting proteins with detergent and preparing GUVs. On the right, the formation of native membranes from cell-derived GPMVs is depicted, beginning with cell preparation and GPMV formation. Central steps common to both methods include chip preparation via plasma cleaning and buffer equilibration, followed by bilayer preparation, where GUVs or GPMVs are added to the chip and incubated. The final stage involves bilayer characterization, assessing unilamellarity using α-hemolysin, lipid diffusion and protein diffusion. Approximate times required for each step are indicated in parentheses.

valuable insights into the dynamics of exocytosis. However, a notable limitation of SLBs is their tendency to adhere to the substrate, which restricts the natural mobility of membrane proteins. This adherence reduces the overall physiological relevance of the results.

In contrast, the SLIM platform eliminates substrate-associated artifacts by providing a free-standing membrane, offering a more biologically faithful platform for studying membrane fusion and protein dynamics. The SLIM system allows proteins to move freely within the membrane,

mimicking their natural behavior in vivo. This model also provides access to both the outer and inner leaflets of the lipid bilayer, enabling the study of multipass transmembrane proteins and extended cytoplasmic domains that would otherwise be restricted in SLBs. Additionally, the horizontal geometry of the SLIM platform is ideal for high-resolution microscopy, allowing for detailed imaging of vesicle docking, undocking and fusion processes.

The free-standing planar geometry of SLIM ensures greater protein mobility, leading to higher efficiency in vesicle docking, priming and fusion events compared with SLBs, BLMs or nanodisc fusion systems. The system's flexibility in incorporating purified proteins or cell-derived membranes from giant plasma membrane vesicles (GPMVs) allows researchers to recreate various cellular environments, enhancing its utility across multiple disciplines. The horizontal geometry of SLIM also enables high-resolution methods, such as laser scanning confocal microscopy with a resonance scanner or total internal reflection fluorescence (TIRF) microscopy, which can precisely monitor biological processes occurring on the lipid bilayer with a high signal-to-noise ratio. Additionally, the SLIM platform's single-molecule imaging capability represents a major technological advancement, allowing dynamic monitoring of protein interactions, single-molecule counting and the participation of multiple proteins in real-time fusion processes.

Limitations

The SLIM platform, developed for in-depth studies of cellular processes at the plasma membrane, offers considerable strengths in membrane visualization and simulating near-physiological conditions. However, certain limitations exist regarding the accessibility of membrane components on the outer leaflet, especially when using native plasma membranes. These limitations do not apply to reconstituted GUV systems where proteins can orient in both directions offering greater flexibility for experimental design.

Orientation and accessibility of membrane leaflets

A key challenge in the current SLIM platform arises from the fixed orientation of the membrane when planar bilayers are formed from GPMVs on the chip. In this process, the inner leaflet of the membrane faces upward while the outer leaflet faces downward into the underlying holes of the substrate. This orientation limits experimental designs that require direct interaction with the outer leaflet since it becomes inaccessible after bilayer formation. Introducing ligands or interacting molecules directly to the outer leaflet after formation is particularly challenging under these conditions. As a result, ligands or other desired molecules must be introduced to the chip before the bilayer is formed. To overcome this limitation, future designs of the SLIM platform are expected to incorporate flow channels. These channels would provide access to both membrane leaflets, allowing for greater flexibility in experimental manipulation and enabling interactions with both the outer and inner leaflets after bilayer formation. This enhancement would substantially broaden the experimental potential of the platform allowing researchers to perform more complex assays on both sides of the bilayer and expanding the range of applications.

Variability in GPMV composition

A key limitation of GPMVs is the selective localization of fusion sites. In GPMVs, fusion tends to occur at specific regions of the membrane rather than being uniformly distributed, leading to reduced vesicle docking. This selective area-based docking probably results from the heterogeneous composition of GPMVs, which retain some of the organizational complexity of native cell membranes, including lipid rafts and other microdomains. In contrast, GUVs exhibit a more uniform distribution across the membrane, lacking the complexity and organization of native membranes. Despite differences in docking behavior and selective fusion sites in GPMVs, the fusion kinetics remain similar between GPMVs and GUVs. This suggests that GPMVs provide a more complex and realistic environment for docking. The bulk collection of GPMVs for bilayer formation can result in the dilution of certain proteins or lipid domains, potentially leaving some bilayers without key components. To address this, future strategies may involve using protein tags and affinity sorting to selectively enrich GPMVs of interest or generating GPMVs from specific regions of the plasma membrane to ensure desired components are present.

Visualization challenges due to silicon substrate

The employment of silicon in the SLIM setup limits observation to regions where the membrane is suspended. This limitation obscures the bilayer sections that overlay the silicon, creating challenges when the area of interest includes proteins or domains located on the supported part of the bilayer. Modifying the silicon structure, such as altering the dimensions and spacing of the holes, can offer a partial solution. A more comprehensive approach would entail design changes that permit dynamic adjustments of the membrane's suspension and support within the system.

Despite these limitations, the SLIM platform represents an important advancement in studying membrane-associated phenomena. These challenges underscore the importance of ongoing development and refinement. Future enhancements will aim to increase the accessibility of membrane components, guarantee the presence of specific proteins or lipids within the bilayers and improve the overall visibility across the entire membrane structure. This continual evolution will ensure the platform remains at the forefront of membrane biology research.

Experimental design

When designing an experiment, the choice between synthetic lipid reconstitution and GPMV-based bilayers depends on the properties of the protein being studied. If the protein can be expressed, purified and reconstituted, a synthetic lipid system is ideal for controlled biochemical and biophysical studies. However, if the protein cannot be easily expressed and purified, requires a specific orientation or functions as part of a complex, a GPMV-based bilayer preserves native asymmetry, lipid composition and protein interactions. Here, we outline the key considerations, including fluorescent labeling, optimization and validation, cell line selection and expertise required to ensure reproducibility.

Selection of fluorophores

Selecting appropriate fluorophores that have high brightness and strong photostability for labeling proteins and lipids is critical for visualizing dynamics in the membrane system. Small organic dyes such as Alexa Fluor, Cy3/Cy5 and ATTO series offer superior stability compared to fluorescent proteins (for example, GFP, mCherry), which tend to bleach faster. For protein labeling, options include genetic fusions (for example, GFP-tagging) or chemical conjugation using NHS-ester or maleimide dyes. Chemical labeling provides brighter, longer-lasting signals and ensures minimal impact on protein function. For lipid labeling, membranes can incorporate commercially available fluorescent lipid analogs that can be easily photobleached (for example, NBD-PE and ATTO 465). When using labeled lipids, it's important to choose analogs that behave similarly to the native lipids (for example, in phase behavior and bilayer stability) and to use a low label fraction (0.5–3%) to avoid altering bulk membrane properties. To reduce photobleaching, use oxygen scavenging systems (glucose oxidase, catalase) and minimize laser exposure. For single-molecule imaging in TIRF microscopy, bright and stable organic dyes in the far-red range (such as Alexa 647, Cy5 or ATTO 647N) are recommended. Studies that require dual-color single-molecule assays use a blue–far-red pair such as Alexa 488 with Alexa 647 for, or a green–red pair such as ATTO 532 with Alexa 647, to exploit spectral separation. For single-vesicle fusion assays, far-red ATTO dyes are preferable due to their enhanced photostability. By carefully choosing fluorophores and optimizing labeling, multicolor images of proteins and lipids in the planar membrane provide reliable observation of protein dynamics and fusion events.

Fluorophore control: lipid-tagged dyes in the 488 nm channel (ATTO 465-DOPE) tend to oxidize even when stored at −20 °C. When this happens, they emit broadly in the Cy3 and Cy5 channels. To ensure accurate signal interpretation, single-fluorophore controls should be performed regularly to characterize dye behavior. Maintaining clean surfaces is essential, and where possible, lipids should be aliquoted immediately after dissolution in a chloroform/methanol mixture to prevent oxidation and variability between experiments.

Selection of cell lines for GPMV production

Generating GPMVs with physiologically relevant lipid composition, protein content and native asymmetry begins with careful selection of the cell line. Membrane properties vary across cell

types, influencing lipid composition, protein distribution and vesicle yield. For this protocol, we validated INS1 (insulinoma) and N2A (neuroblastoma-derived) adhesion cell lines, alongside ExpiHEK293 suspension cells, ensuring the preservation of native membrane properties. INS1 cells serve as a model for endocrine membranes, N2A cells retain neuronal traits and ExpiHEK293 cells offer high transfectability for customizable protein incorporation. The choice of cell line directly impacts the biological relevance of the reconstructed membranes, ensuring compatibility with specific experimental goals.

Optimizing GPMV formation requires precise control over cell density, vesiculation buffer composition and incubation time. Adhesion cells should be grown to 80–90% confluency, while suspension cells must be maintained at optimal density. Chemical vesiculation conditions must be optimized per cell type to balance yield and membrane integrity. Prolonged exposure to vesiculation agents can compromise membrane structure. High-quality GPMVs should be uniform, free of cellular debris and exhibit phase behavior consistent with physiological membranes, as assessed by fluorescence microscopy.

Preserving membrane asymmetry is essential for capturing physiologically relevant membrane dynamics. At the GPMV level, asymmetry can be assessed using fluorescence quenching assays with NBD-labeled lipids and sodium dithionite to selectively quench outer leaflet fluorescence, while annexin V binding confirms phosphatidylserine exposure. Membrane phase separation studies using Laurdan or DiI fluorescence provide further validation of leaflet-specific lipid organization. Functional assays, including receptor–ligand interactions and antibody-based protein orientation verification, can be used to confirm protein topology in GPMV and the planar membrane format. By integrating precise cell line selection, optimized GPMV formation and rigorous asymmetry validation at both the vesicle and bilayer levels enable the faithful reconstruction of native membrane landscapes.

Optimization and validation

Every experimental condition must be rigorously validated to ensure the system functions as intended. To confirm the formation of a continuous and fluid bilayer, we use fluorescence recovery after photobleaching (FRAP), where a small region of the fluorescent membrane is photobleached and fluorescence recovery is monitored over time. The fluorescence recovery indicates the lateral diffusion of lipids and proteins, confirming membrane fluidity. A well-formed suspended membrane should exhibit fluorescence recovery, consistent with diffusion in a fluid lipid bilayer. If FRAP shows no recovery, it suggests the membrane might not be fully connected between holes. Membrane stability and fluidity are highly dependent on lipid composition and ratio. A common approach is to use a mixture of unsaturated phosphatidylcholines for fluidity and cholesterol to enhance mechanical stability, ensuring the bilayer remains both stable and fluid. To validate single-molecule imaging conditions, we use single-step photobleaching using single-stranded DNA as a reference. Alternatively, fluorescence correlation spectroscopy can also be used to measure diffusion coefficients and molecular concentrations within the membrane.

For membrane fusion assays, appropriate controls are included to verify protein functionality. To confirm that observed fusion events, such as lipid or content mixing, are mediated by the fusion machinery, we incorporate negative controls where key fusion proteins are omitted or replaced with mutant variants, such as the non-functional V-SNARE mutant VAMP4x[35]. The protein-to-lipid ratio in reconstituted membranes is another critical variable, as it influences membrane behavior and fusion efficiency. We use existing quantitative protein copy number estimates on the synaptic vesicle[36], though this value may vary depending on experimental conditions. Finally, performing an activity assay after reconstitution helps ensure that the protein remains correctly folded and functionally intact.

Required expertise

This protocol is accessible to researchers with limited experience in membrane biophysics or fluorescence microscopy. A basic understanding of lipid bilayer properties, membrane–protein interactions and fluorescence imaging will aid in experimental design and data interpretation. A basic skill set in cell culture, passaging cells and treatment of cells for GPMV

formation, fixation end so on is required to collect GPMVs. Familiarity with diffusion dynamics, membrane fusion mechanisms such as SNARE-mediated fusion, and imaging techniques such as FRAP and single-molecule tracking is beneficial for selecting appropriate controls and optimizing measurements. Technical proficiency in lipid handling is essential, including vesicle preparation via GUV or GPMV induction. Fluorescence microscopy skills, particularly in confocal and TIRF imaging, are required for optimizing laser settings and fluorophore selection. Single-molecule studies benefit from expertise in noise reduction, photobleaching analysis and camera calibration. Fluorescence image analysis is a key component of this protocol. Researchers should be familiar with software such as ImageJ/Fiji for FRAP analysis and for single-particle tracking. While suitable for newcomers, prior experience with model membranes, lipid reconstitution and high-resolution microscopy enhances efficiency and reproducibility. Hands-on training in vesicle preparation, imaging and data analysis through workshops or collaborations will further support successful implementation.

Materials

Biological materials

Cell lines (available from the corresponding author upon request)

- Rat insulinoma cell line INS-1 832/3 (Millipore Sigma, cat. no. SCC208) https://scicrunch.org/resolver/CVCL_7226
  Mouse Neuro-2a (N2A) cells (ATCC, cat. no. CCL-131) https://scicrunch.org/resolver/CVCL_0470
  ▲ **CAUTION** The cell lines used in your research should be regularly checked to ensure they are authentic and are not infected with mycoplasma.

Proteins

- Pre-assembled t-SNAREs (mouse SNAP25b/rat STX1A) (see 'Reagent setup')
- Mouse VAMP2 (see 'Reagent setup')
- Rat synaptotagmin 1 (SYT1) residues 57-421 (see 'Reagent setup')
- Human complexin 1 (see 'Reagent setup')

Reagents

- Ni-NTA agarose (Thermo Fisher, cat. no. 30230)
- Imidazole (Thermo Fisher, cat. no. I5513)
- Glycerol (J.T. Baker, cat. no. 2136-03)
- TEV protease (Sigma-Aldrich, cat. no. T4455)
- SUMO protease (Life Technologies, cat. no. 12588-018)
- Bio-Rad protein assay kit (Bio-Rad, cat. no. 500-0001)
- Laemmli Loading Buffer, 4× (Bio-Rad, cat. no. 1610747)
- Tris–glycine SDS running buffer, 10× (Bio-Rad, cat. no. 1610772)
- Mini protean TGX Stain free protein Gels, 10 well, 50 µL (Bio-Rad, cat. no. 4868094)
- Precision Plus Protein WesternC blotting standards (Bio-Rad, cat. no. 1610385)
- Trans-Blot Turbo RTA Mini 0.2 µm Nitrocellulose Transfer Kit (Bio-Rad, cat. no.1704270)
- Precision Plus Protein Dual Color Standards (Bio-Rad, cat. no. 1610374)
- Bio-Safe Coomassie stain (Bio-Rad, cat. no. 161-0786)
- ImageJ free software (US National Institutes of Health)
- MatLab (Mathworks)
- Milli-Q water
- VAMP2 mouse antibody (ProteinTech, cat. no. 67822-1-1g)
- Synaptophysin mouse antibody (ProteinTech, cat. no. 67864-1-1g)
- 35 mm glass-bottom dishes (MatTek, cat. no. P35G-1.5-14-C)
- Norland Optical adhesive 61 (NOA 61; Thorlabs, cat. no. NOA61)
- Sticky-Slide 8-well high (Ibidi, cat. no. 80808)

- Sticky-Slide 18 well (Ibidi, cat. no. 81818)
- Anhydrous DMSO (Thermo Fisher, cat. no. D12345)
- Alexa Fluor 647 C2 Maleimide (Thermo Fisher, cat. no. A20347)
- Alexa Fluor 647 NHS Ester (Succinimidyl Ester) (Thermo Fisher, cat. no. A20006)
- Pierce dye removal columns (Thermo Fisher, cat. no. 22858)
- Amersham NAP 5 columns (Cytiva, cat. no. 17085301)
- RBS 50 solution (Millipore Sigma, cat. no. 83462-1L)
- Sepharose CL-4B resin (Cytiva, cat. no. 17015001)

Lipids

▲ **CAUTION** Please note that all lipid stocks are stored in chloroform, which poses a chemical hazard. Avoid inhaling gases, fumes, vapors or sprays. It is essential to wear appropriate protective gear when handling these materials. Ensure that all work involving chloroform is carried out within a fume hood.

▲ **CRITICAL** Lipids are purchased in chloroform solution from Avanti Polar Lipids and should be kept at −20 °C for optimal preservation. Special attention is required for the storage of lipid stocks, especially for hygroscopic varieties such as 1,2-dioleoyl-sn-glycero-3-phospho-L-serine (DOPS) and L-α-phosphatidylinositol-4,5-bisphosphate (PI (4,5) P2). These compounds are susceptible to precipitation if the containers are not sealed properly.

- DOPS; Avanti Polar Lipids, Cat. no. 840035)
- 1,2-Dioleoyl-sn-glycero-3-phosphocholine (DOPC; Avanti Polar Lipids, cat. no. 850375)
- L-α-Phosphatidylinositol-4,5-bisphosphate (brain, porcine, ammonium salt) (PI(4,5)P2 or PIP2), brain extract, $CHCl_3$/CH_3OH/H_2O (20:9:1) stock, Avanti Polar Lipids, cat. no. 840046X
- 1,2-Dioleoyl-sn-glycero-3-phosphoethanolamine-*N*-(7-nitro-2-1,3-benzoxadiazol-4-yl) (ammonium salt) (NBD-PE; Avanti Polar Lipids, cat. no. 810145)
- ATTO 647N-DOPE (Attotec, cat. no. AD 647N-161).
- ATTO 488-DOPE (Attotec, cat. no. AD 488-161)

SUVs

- Bond Breaker TCEP solution (Thermo Scientific, cat. no. 77720)
- Potassium chloride (Sigma-Aldrich, cat. no. P9541)
- HEPES (Fisher- Bioreagent, cat. no. BP 310)
- Dithiothreitol (DTT) (RPI, cat. no. D11000)
- Triton-X-100 (Sigma, CAS 9036-19-5)
- *N*-Octyl-β-D-glucopyranoside (OG; Chem Impex Intl, cat. no. 00234)
- Bio-BeadsT SM2 Adsorbent Media (Bio-Rad, cat. no. 152-3920, 20-50 Mesh)
- OptiPrep (Stemcell Technologies, cat. no: 07820).
- Chloroform (American Bioanalytical, cat. no. AB00350)
- EDTA (Sigma-Aldrich, cat. no. EDS)
- *n*-Dodecyl-β-maltoside (Thermo Scientific, cat. no. 89903)
- Sulforhodamine B (Invitrogen, cat. no. S1307)
- Mini dialysis cassette 7,000 Da molecular weight cutoff (MWCO) (Thermo Scientific, cat. no. 69592)

GPMVs

- *N*-Ethylmaleimide (NEM) (Calbiochem, cat. no. 34115)
- Sucrose (Fisher, cat. no. S-500 -210554)
- MemGlow 488 (Cytoskeleton, cat. no. MG01-02)
- Calcium chloride (Sigma-Aldrich, cat. no. C5080)

Equipment

Cell culture

- Inverted contrast microscope for routine examination of cell cultures
- Water bath at 37 °C to warm cell culture media

- Incubator at 37 °C with 5% CO_2
- Greiner centrifuge tube, 50 mL (Sigma-Aldrich, cat. no. T2318)
- Cell culture dishes 100 mm (Corning, cat. no. 430167)
- Filtered sterile pipette tips (Fisher Scientific, cat. no. 02-707-404)
- Pipet-Aid (Drummond, cat. no. 4-000-101)
- Serological pipettes (Corning, 10, 25 and 50 mL)
- Scissors (Fisher Scientific)

Proteoliposomes

- Autoclave (LBR Scientific LCC, TUTTNAUER)
- Shaker Incubator at 37 °C for *E. coli* growth (Eppendorf, model no. Innova-44R)
- Magnetic stirrer (VWR)
- High-speed centrifuge (Eppendorf, model no. 5427R)
- Low-speed centrifuge for 15/50 mL tubes (Eppendorf, model no. 5702-R)
- Ultracentrifuge (Optima L-90k ultracentrifuge, SW60 Ti rotor; SW55 rotor; JS5.0 rotor Beckman)
- Table Spin centrifuge (Argos Flexifuge)
- pH meter (Fisher Scientific, model no. AB15)
- Refrigerator (−80 °C) (Haier, model no. HYCD-290)
- Refrigerator (4 °C and −20 °C) (Haier, model no. DE-25W262)
- Microcentrifuge tube 1.7 mL (Posi-Click Denville, model no. 1149K01)
- Microcentrifuge tube 0.6 mL (Posi-Click Denville, model no. C-2176)
- Serological pipette 5 mL (Falcon, cat. no. 357543)
- Serological pipette 10 mL (Falcon, cat. no. 356551)
- Serological pipette 25 mL (Basix, cat. no. 20210904-071-B)
- 10 mL Petri dish (VWR)
- Heating Block (VWR Scientific Products)
- Cell Spreader (VWR)
- Water Bath (Fisher Scientific)
- High-capacity centrifuge (Beckman J-HC, cat. no. 367501)
- JS 5.0 liner (Beckman Coulter, cat. no 368735-40)
- D-tube dialyzer, 6–8 kDa MWCO (Novagen, cat. no. 71509-3)
- Centrifuge tubes, 5 × 41 mm, 0.8 mL open-top thinwall ultraclear tube (Beckman Coulter, cat. no. 344090)
- Amicon Ultra-0.5, 30 kDa membrane (Millipore, cat. no. UFC503096)
- PVDF membrane, 0.2 µm (Macherey-Nagel, cat. no. 740401.50)
- FluoroNunc Maxisorp 96-well white plate (Thermo, cat. no. 437591)
- Poly-Prep chromatography columns (Bio-Rad, cat. no. 731-1550)
- Glass tube, 12 × 75 mm (Fisher, cat. no. 14-961-26)
- Vacuum desiccator (VWR)
- Vacuum pump (Alcatel 2005 C1, ultimate vacuum $<10^{-4}$ mbar)
- Weighing balance (Mettler Toledo, ML300ZE, and VWR, VWR-64B2)
- Gas-tight glass syringe (Hamilton, cat. nos. 1701RN, 1710 RN, 1750 RN)
- SpectraMax M5 multimode microplate reader (Molecular Devices, model no. Flex Station3)
- Digital vortex mixer (VWR, cat. no. 14005-824)
- Liquid chromatography system (ÄKTA Explorer; GE Healthcare)
- Superdex 200 10/300 GL prepacked column
- Empty chromatography column (Bio-Rad Econo-Column or equivalent)
- Orbital shaker (Barnstead Lab, multipurpose rotator, model no. 2314Q)
- Harrick Plasma Basic Plasma Cleaner (Harrick Scientific Corporation, PDC 32G)
- Nitrogen tank and pressure gauge
- Automatic high sensitivity osmometer (Precision Systems, model no. 5004 Micro-Osmette)

Microscopy

▲ **CRITICAL** There is a diverse range of hardware and acquisition software available, allowing for various effective combinations. We describe our specific setups below, this protocol can be adapted to any microscope system that includes a minimum of two laser lines, two fluorescence channel detectors, an electron-multiplying charge-coupled device (EMCCD) camera and an enclosure capable of regulating temperature.

Confocal microscope

Inverted confocal laser-scanning microscope (Leica SP8) equipped with a GalvoZ stage.
The following parts of the microscope are necessary to perform membrane fusion experiments.

- Objectives (Leica, model no. HC PL APO 40×/1,10 W CORR CS2 with 0.65 mm long working distance is required for imaging the lipid bilayer)
- Lasers: argon (488 nm) and helium–neon (HeNe; 633 nm)
- Detectors: 3× spectral photomultiplier tube (PMT) and 1× transmission PMT for bright-field microscopy, differential interference contrast and polarization, respectively
- Microscope enclosure with temperature control
- GalvoZ stage with inserts for slides and 35 mm dishes.

TIRF microscope

- A Nikon Ti-E Sapphire fully motorized body (Nikon Instrument, Japan) with a perfect focus system
- Nikon immersion oil type F (MXA22168)
- Electron-multiplying charge-coupled device camera (Andor IXON 887)
- Lasers (488 nm, 532 nm and 633 nm, Spectra-Physics)
- Dual view opto-split suitable for collecting fluorescence from 488 and 633 nm channels.
- A Plan Apo 60× numerical aperture (NA) 1.45 objective lens (Nikon Instruments)
- Acquisition software: NIS-Elements AR 5.30.02 (Nikon)
- The optical configuration should be set according to the dyes used.

Equipment setup

Preparation of silicon chips

The manufacturing process for all silicon chips has been optimized and standardized, and the products are readily available for purchase from Micromotive. Detailed designs can be found in Fig. 1 and Supplementary Material.

Preparation of BSA-coated coverslips and chambers

Incubate MatTek glass-bottom dishes in 1 mL of a 1 mg/mL BSA solution for 1 h. Wash two times with GPMV buffer. Coat immediately before use.

Preparation of silicon chips for confocal microscopy

Silicon chips are glued on a glass coverslip using optical transparent glue NOA61 to fit in an Ibidi Sticky-Slide 8 Well high. See the 'Procedure' for more details.

Preparation of silicon surface for TIRF microscopy

Silicon chips of thickness 4.7 µm are attached to a Ibidi Sticky-Slide 8 well in a format. See the 'Procedure' for more details.

Confocal microscopy with incubation systems

We include here instructions for setting up the Leica confocal microscope for image acquisition. These steps and setting could be adapted to other similar systems.

1. Turn on the temperature control within the microscope enclosure to maintain the sample at 37 °C.
2. In 'configuration', turn on the argon (488 nm) and HeNe (633 nm) lasers.

3. Activate PMT 1, tick 'visible', set laser power to 2% and spectral range to 500–550 nnm, click 'PMT 1' and set gain to 800 (change this later depending on signal strength).
4. Activate PMT 2, tick 'visible', set laser power to 5% and spectral range to 650–700 nm, click 'PMT 2' and set gain to 800 (change this later depending on signal strength).
5. Activate TMD, tick 'visible', set gain to 250 (change this later depending on signal strength).
6. In 'Acquire' → 'Acquisition':
   - Set 'Acquisition mode' to XYT
   - Set 'Format' to 512 × 512
   - Set 'Speed' to 1,800 or 8,000 Hz (change this depending on the experimental requirement)
   - Set 'Time interval' to Minimize

   Set 'No of Frames' to 5,000

TIRF microscopy with incubation systems

We include here instructions for setting up the Nikon TIRF microscope for image acquisition. These steps and settings could be adapted to other similar systems.

1. Turn on the microscope and required laser lines (for example, 488, 532 and 647 nm).
2. Select the 60× TIRF oil objective and put a drop of Nikon immersion oil type F (index of 1.518 at 23 °C).
3. Place the SLIM chip with a slide holder.
4. Turn on the light and focus the array of holes on the chip.
   ▲ **CRITICAL** The SLIM chip is easier to focus with the bright light in epifluorescence mode.
5. Switch off the bright light and turn on the required laser line.
6. Change the setting to TIRF mode.
   ▲ **CRITICAL** The TIRF angle maybe 2–3° different than the corresponding glass slide. Therefore, it may need initial scanning to find the exact TIRF mode.

   For simultaneous dual color monitoring, insert the corresponding dual viewer/optosplit to split the beam.

Reagent setup

t-SNAREs (mouse SNAP25, rat STX1A)

t-SNARE proteins can be expressed using a vector, pTW34, as previously described[25,26,37,38]. After purification, aliquot the protein and flash-freeze in liquid nitrogen, using a buffer containing 400 mM KCl, 25 mM HEPES, 1% (wt/vol) OG, 1 mM DTT and 10% (v/v) glycerol, with the pH adjusted to 7.4. For long-term storage, up to 6 months, keep the protein at −80 °C. Proteins can be labeled to a high degree using Alexa Fluor 647 NHS ester. Solubilize dye in anhydrous DMSO and mix the protein and dye in 1:5 molar ratio and label for 30 min. Quench the reaction by adding 1 M Tris. Remove excess dye using dye removal columns.

6×-His-SUMO-VAMP2

Express and purify full-length, wild-type mouse VAMP2 as previously described[39]. After purification, aliquot the protein and flash-freeze in liquid nitrogen, using the same buffer as for t-SNARE proteins (400 mM KCl, 25 mM HEPES, 1% (wt/vol) OG, 1 mM DTT and 10% (v/v) glycerol). Store at −80 °C for up to 6 months.

Synaptotagmin 1-5×His

The rat SYT1 protein used in this assay is a truncated version (residues 57–421 followed by 5× His, pLM6, PMID: 12119360), including the transmembrane domain and the entire cytosolic domain. Expression and purification have been previously detailed[27]. After purification, aliquot the protein and flash-freeze in liquid nitrogen, using the same buffer as described above and store at −80 °C for up to 2 months.

▲ **CRITICAL** The salt concentration in the storage buffer affects the solubility and stability of proteins, so it should be optimized for each specific protein. A salt concentration of 400 mM, combined with 1% OG, is ideal for maintaining the solubility and stability of these membrane proteins during storage.

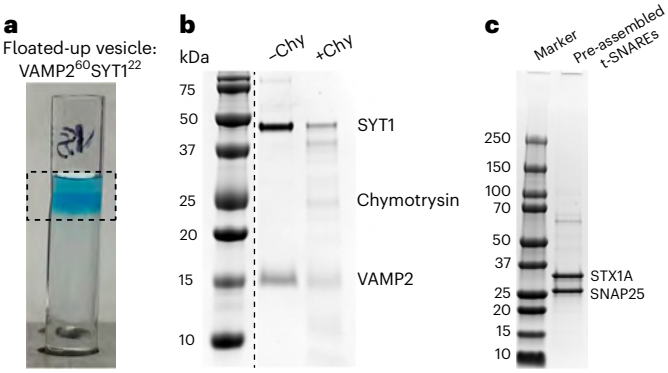

Fig. 3 | Vesicle and bilayer reconstitution. a, Float-up of VAMP2^{60}SYT1^{22} vesicles (superscript numbers denote the copy number of proteins per vesicle, as described in Step 16). After reconstitution with corresponding proteins and overnight dialysis, vesicles were floated up through a gradient of 30%, 20% and 0% Optiprep density medium. Vesicles labeled with DOPE ATTO 647N (blue) reach the 0% layer as shown in the dotted line box. **b**, SDS–PAGE gel run of v-SNARE VAMP2 and SYT1-incorporated vesicles after vesicle float-up. Chymotrypsin (Chy) treatment removes all proteins facing outside the vesicle demonstrating orientation of incorporated proteins. **c**, SDS–PAGE of the liposome containing t-SNAREs.

Complexin 1

Human complexin 1 can be expressed as previously described[40,41]. After purification, aliquot the protein and flash-freeze in liquid nitrogen in a buffer containing 140 mM KCl, 25 mM HEPES, 1 mM TCEP and 10% (vol/vol) glycerol. Store at −80 °C for up to 6 months. Do not thaw and r-freeze aliquots. Complexin 1 can be labeled using maleimide chemistry due to the presence of a single cysteine residue and its function is not affected by labeling. Following the manufacturer's protocol, solubilize dye in anhydrous DMSO and mix complexin and dye (1:5 molar ratio, respectively) and label overnight at 4 °C with gentle rotation. Excess dye is removed with a dye removal column using a resin volume based on protein volume (for example, 100 µL resin for 100 µL protein). Further cleanup can be done by running protein through a NAP-5 column from Cytiva.

Reconstituted SUVs (V-SUVs and V-SYT1 SUVs)

Prepare SUVs using DOPC/DOPS/ATTO 647N in a molar ratio of 77:20:3. For VAMP2-SUVs (vSUVs), maintain a final protein:lipid ratio of 1:200. For VAMP2-synaptotagmin 1 SUVs (SYT1-vSUVs), set the VAMP2/SYT1 final protein:lipid ratio to 1:200:500. For detailed instructions, refer to the 'Preparation of SUVs' section in the 'Procedure'.

▲ **CRITICAL** The protein-to-lipid ratio can be adjusted depending on the experiment. Protein size and other factors influence reconstitution efficiency and orientation. Standardize carefully for each reconstitution system, as protein input varies based on these parameters. In our assay, SNAREs and SYT1 achieve 50–60% incorporation efficiency, with 50–55% of the reconstituted liposome proteins facing outward, as determined by chymotrypsin protection analysis (Fig. 3). The initial protein input is adjusted accordingly, and reconstitution methods are well-characterized elsewhere[42].

GPMV buffer (10 mM HEPES, 150 mM KCl, 2 mM $CaCl_2$, 10 mM sucrose, pH 7.4)

Mix 18.75 mL of KCl (2 M stock), 0.5 mL of $CaCl_2$ (1 M atock), 2.5 mL of HEPES (1 M stock pH 7.4) and 5 mL of sucrose (0.5 M stock) in distilled water and bring to 250 mL. This buffer can be stored at room temperature (22 ± 2 °C) or 4 °C for up to 6 months.

▲ **CRITICAL** Sucrose is essential to burst GUVs

GPMV working buffer (2 mM NEM)

Dissolve 2.5 mg NEM in 10 mL of GPMV buffer. The solution should be freshly prepared.

Dialysis buffer A (5×)

Prepare 2 L of buffer containing 600 mM KCl, 125 mM HEPES and 5 mM DTT, adjusted to pH 7.4. This buffer should be freshly prepared.

Dialysis buffer A (1×)

Take 1 L of buffer A (5×) and dilute it to 5 L with Milli-Q water. Since this buffer contains DTT, prepare it just before use.

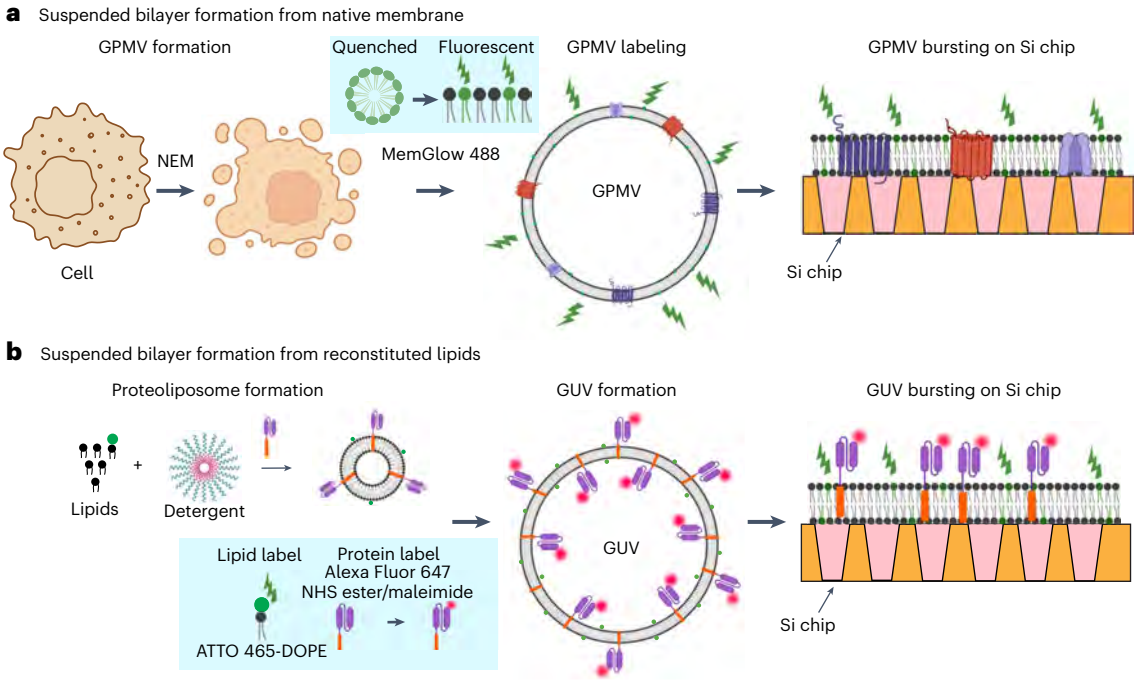

Fig. 4 | Schematic representation of the labeling methods. a, The native planar bilayer is visualized by labeling GPMVs with MemGlow 488. Inset: MemGlow dye is quenched/low fluorescence until it embeds in a lipid bilayer and becomes brightly fluorescent. **b**, A schematic representation of labeled lipids or protein used in the reconstituted fusion system. For bilayer visualization, ATTO 465-DOPE (lipid) or NHS ester-conjugated Alexa 647 (protein) was used.

t-SUV reconstitution buffer

Freshly prepare 2 mL of dialysis buffer A (5×) and add 20 mg OG to achieve a final concentration of 1% (wt/vol).

v-SUV reconstitution buffer

Freshly prepare 2 mL of dialysis buffer A (1×) and add 20 mg OG to achieve a final concentration of 1% (wt/vol).

MemGlow 488: fluorogenic membrane probe solution (20 µM)

For creating a 20 µM stock solution, reconstitute the lyophilized powder (2 nmol) in 100 µL of anhydrous DMSO. Aliquot the stock into 5 µL portions and store at −80 °C for up to 3 months.

Procedure

Preparation of GUVs

▲ **CRITICAL** All the lipid and protein dyes used in these experiments are schematically shown in Fig. 4.

● **TIMING 2–3h**

1. Use option A to prepare giant plasma membrane (cell-derived) vesicles and option B to prepare synthetic GUVs from SUVs with proteins of interest. See Fig. 3 for a characterization of the proteo-SUVs.

   (A) **Preparation of GPMVs**

   ▲ **CRITICAL** This procedure has been tailored for cells cultured in 100 mm diameter cell culture dishes. The yield of GPMVs is influenced by factors such as cell quantity, incubation time and temperature. Optimal results are achieved with an incubation

time of 1 h and 30 min, but these parameters should be fine-tuned for each specific cell type. The conditions outlined here have been successfully applied and validated in various cell lines, including INS1, N2A, HEK293, HeLa and HUVEC.

(i) Culture the cells in a 100 mm dish until the cells reach 80% confluency (1–2 days). Refer to the ATCC database at (http://www.atcc.org/) or refer to the guidelines provided by the supplier to determine the suitable conditions and media for use.

(ii) Remove the cell culture media and wash the cells three times with 5 mL of PBS, followed by 5 mL of GPMV buffer.

(iii) Add 1 mL of GPMV working buffer to the cells and incubate for 1 h 30 min. (Optional) While this protocol uses NEM to maintain protein functionality, the same process can be carried out using 25 mM paraformaldehyde and 2 mM DTT to produce GPMVs.

(iv) Transfer the GPMV-rich cellular supernatant into a microcentrifuge tube using cut pipette tips.

■ **PAUSE POINT** After isolation, GPMVs can be stored at 4 °C or on ice for transfer to the silicon chip.

◆ **TROUBLESHOOTING**

(v) (Optional) For microscopic visualization, GPMVs can be labeled by incubating with MemGlow 488 Fluorogenic Membrane Probe Solution at a concentration of 2–20 nM. Afterward, place the labeled GPMVs onto BSA-coated MatTek glass-bottom dishes for confocal microscopy imaging.

(B) **Preparation of GUVs from SUVs**

(i) In a chloroform-rinsed glass tube, mix DOPC, DOPS, PIP2 and ATTO 465 in a molar ratio of 76.5:20:3:0.5, targeting a final concentration of 7 mM in a 50 µL volume. Dry the mixture under a stream of nitrogen to remove the solvent. Ensure the glass tubes are wrapped in aluminum foil to protect the fluorescent lipids from light.

▲ **CRITICAL STEP** The amount of lipids can be adjusted depending on the experimental needs.

(ii) Rehydrate the dried lipids by adding t-liposome reconstitution buffer (~1% OG) and t-SNARE proteins to achieve a protein:lipid ratio of 1:800, bringing the total volume to 50 µL.

▲ **CRITICAL STEP** The protein-to-lipid ratio can be adjusted depending on the specific experiment.

▲ **CRITICAL STEP** Do not use protein aliquots if any precipitation is observed after thawing.

(iii) Vortex the mixture for 15 min at room temperature to ensure proper mixing.

(iv) Dialyze the solution against 1 L of dialysis buffer A overnight at 4 °C.

(v) The next day, collect the t-SUVs and store at 4 °C

■ **PAUSE POINT** SUVs can be stored at 4 °C for up to 2–3 days.

(vi) Add sucrose to the t-SUV solution to achieve a final concentration of 2 mM.

(vii) Deposit a few 2 µL drops of the t-SUV–sucrose mixture onto a MatTek glass-bottom dish and allow the drops to dry at room temperature under atmospheric pressure.

(viii) Rehydrate the dried lipid film spots with 6 µL of deionized water and allow them to dry again under the same conditions. Then, rehydrate the lipid film a second time by adding 10 µL of deionized water and letting it sit for 40–50 min.

◆ **TROUBLESHOOTING**

(ix) Gently pipette up and down 1–5 times using a pipette with a cut tip at the edge of the droplet to collect 10 µL from each droplet. The two droplets can be transferred to the prepared silicon surface.

■ **PAUSE POINT** Multiple drops can be pooled and stored at 4 °C. These are typically stable for up to 7 d if (1) there is no reconstituted protein and (2) no charged lipids are used, for example, PIP2, which might cause aggregation. Discard if you have trouble resuspending the lipids gently with a cut, 1,000 µL tip.

▲ **CRITICAL STEP** The quality of GUVs is better if they are recovered before the 50 min mark.

Cleaning the silicon chip

● **TIMING ~40 min**

2. Add 400 µL of 10% RBS 50 detergent solution to each chip and gently shake for 5–10 min.
3. Rinse the chips under running water for 5 min to remove any residual RBS solution.
4. Thoroughly wash the chips with MiliQ water five times, shaking gently for 1 min each time.
5. Wash with 400 µL of 200-proof ethanol, shake for 1 min and repeat this process three times.
6. Wash with 400 µL of methanol with 1 min of gentle shaking, repeating the process three times.
   ▲ **CRITICAL STEP** Ensure meticulous washing to eliminate any trace of RBS detergent, which can impact subsequent bilayer formation.
7. Discard all solutions and air-dry the chip or incubate it at 37 °C for 15 min.

Formation of planar bilayer on the chip

● **TIMING ~2–3 h**

8. After cleaning and drying the chip, it should be treated for 5 min in a plasma cleaner to clean and activate the surface.
9. Add 400 µL of 200-proof ethanol and incubate for 5 min with gentle rocking. This step helps remove trapped air within the holes.
10. Replace the ethanol with water, carefully avoiding air bubbles entering the chip. Mix water 1:1 (vol/vol) and solvent in the chamber, repeating this process five times.
    ▲ **CRITICAL STEP** After the ethanol wash, keep the chip in water. Do not let it dry as this can introduce air bubbles, preventing smooth bilayer formation.
11. Replace the water with an appropriate buffer.
    - For the confocal chip, water should be replaced with 25 mM HEPES (pH 7.4), 120 mM KCl, 0.2 mM TCEP and 5 mM $MgCl_2$ buffer
    - For the single-molecule SLIM chip, water should be replaced with buffer containing 45% OptiPrep, 25 mM HEPES (pH 7.4), 120 mM KCl, 0.2 mM TCEP and 5 mM $MgCl_2$. This 45% OptiPrep is required to match the refractive index for the TIRF setup.
      ▲ **CRITICAL STEP** A 5 mM $MgCl_2$ supplement is crucial for adhering and bursting the GUV or GPMV on the silicon chip.
12. Cut the end of a 20 µL tip to make the orifice bigger. Gently collect previously prepared GUV or GPMV solution and dispense it onto the silicon chip.
13. Incubate the lipids on the chip for 20 min to form the bilayer. Place the chip in the JS5.3 rotor holder compatible with a Beckman Coulter Avanti centrifuge and centrifuge at 100*g* at room temperature for 5 min.
    ▲ **CRITICAL STEP** This gentle spin helps to settle GUVs/GPMVs and promotes even spreading on the chip.
14. Gently exchange the buffer on the top side of the membrane to remove any unbound GUVs or GPMVs.
    Depending on the chip used, visualize the membranes using a confocal or TIRF microscope.

For the expected result, see Fig. 5.

Preparation of proteoliposomes

● **TIMING ~18–24 h**

15. Mix lipids (see 'Reagent setup') at the desired ratio in glass tubes and evaporate the solvent using nitrogen gas. Remove trace amounts of organic solvent under a high vacuum for 2 h.
16. Hydrate the dried lipids with v-SUV reconstitution buffer containing 1% (wt/vol) OG, which is approximately twice its critical micelle concentration (CMC), to ensure efficient solubilization of lipids and proteins. Add appropriate amounts of protein to achieve the desired copy number per vesicle (for example, ~15–20 copies of SYT1 and ~60–70 copies of VAMP2), adjusting based on reconstitution efficiency.
17. Use option A to prepare proteoliposomes for monitoring both lipid and cargo mixing, and option B to prepare proteoliposomes specifically for lipid mixing.
    (A) **Prepare proteoliposomes for monitoring both lipid and cargo mixing**
    (i) Add sulforhodamine B solution to achieve a final concentration of 50 mM.
    (ii) Vortex the tubes containing solution for thorough component dispersal.

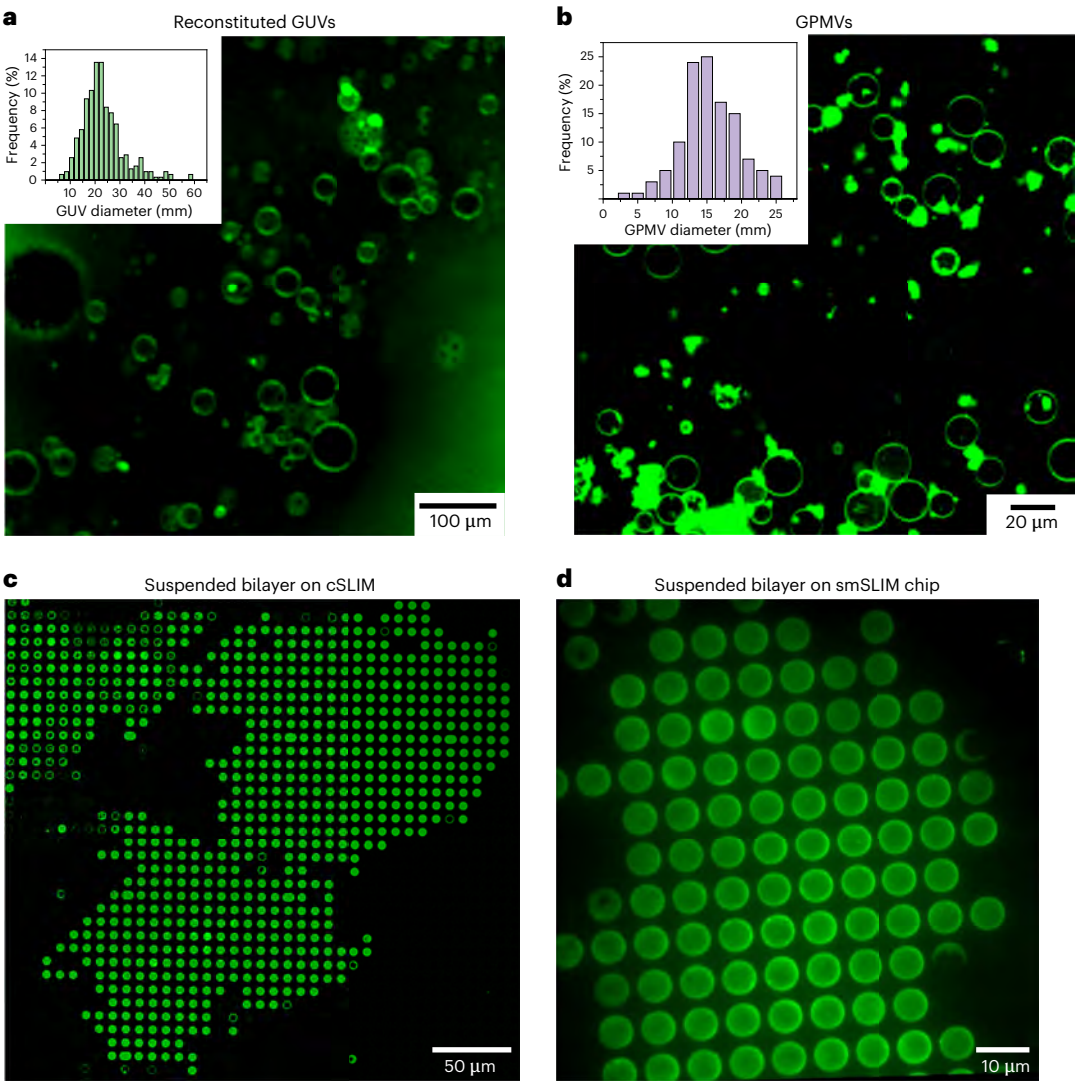

Fig. 5 | Bilayer preparation. a, GUVs containing pre-assembled t-SNAREs are formed after resuspension and imaged with a confocal microscope using a 488 nm laser. Size distributions of the GUVs are shown in the inset. $N > 100$. Scale bar, 100 µm. **b**, GPMVs are formed with NEM treatment of the INS-1 cells and imaged after MemGlow 488 labeling. Similarly, size distributions of GPMVs are shown in the inset. $N > 100$. Scale bar, 20 µm. **c**,**d**, Suspended bilayers with reconstituted GUVs are shown with confocal (**c**) and TIRF chips (**d**). Scale bars, 50 and 10 µm, respectively.

(iii) Add two times the volume of dialysis 1× buffer A to rapidly dilute the detergent concentration below its CMC. Rapid vortexing is necessary while adding the 1× dialysis buffer A. Incubate the solution for 20 min in a mixer.
▲ **CRITICAL STEP** If the detergent concentration does not go below its CMC, then SUV formation and protein incorporation efficiency decline markedly. Rapid dilution also enhances protein incorporation into the vesicle.

(iv) Pass the sample solution through a prewashed and pre-equilibrated CL-4B column.
▲ **CRITICAL STEP** This step is essential for removing detergent, unincorporated protein and unencapsulated sulforhodamine B dye from the protein–lipid–detergent mixture. Proper column preparation is crucial: prewash and equilibrate the CL-4B column thoroughly with vesicle buffer before introducing the sample. After loading, elute with vesicle buffer and collect the purified proteoliposomes.

(B) **Prepare proteoliposomes for monitoring lipid mixing**

(i) Dialyze the collected vesicle solution in a 7 kDa MWCO dialysis cassette using 4 L of dialysis 1× buffer A overnight at 4 °C with 4 g of Bio-Beads.

(ii) The next day, purify the proteoliposomes away from unicorporated protein by floating up through an OptiPrep density gradient.

- Mix dialyzed samples 1:1 (vol/vol) with 60% (vol/vol), then layer 250 µL of 20% (vol/vol) and 50 µL of 0% OptiPrep (all prepared in 1× dialysis buffer A) sequentially on top in a 5 × 41 mm, 0.8 mL open-top thinwall ultraclear tube (Beckman Coulter).
- Centrifuge the gradient in a Beckman SW55 rotor at 48,000 rpm for 4 h at 4–8 °C.

▲ **CRITICAL STEP** Maintain the various layers, which must be carefully overlaid to prevent any disturbance to the interface between them.

(iii) Collect 75 µL of liposomes from the 0–20% interface, aiming for a clean, concentrated fraction. For better results, use the collected SUVs on the same day.

18. Assess the protein incorporation ratio in proteo-SUVs through SDS–PAGE gel electrophoresis and Coomassie blue staining. Load 15 µL of the vesicle solution into the gel initially. If the protein bands appear too faint or overloaded, make volume adjustments and rerun the gel. For the expected result, see Fig. 3. Ensure that the VAMP2-to-synaptotagmin ratio is ~4.6:1.
19. Characterize the size distribution of SUVs by dynamic light scattering or cryo-EM.

Experiment

Vesicle docking and fusion

● **TIMING ~18–24 h**

20. Verify the membrane fluidity using the confocal FRAP module. See Fig. 6 and Supplementary Video 1.
21. Dilute 5 µL of the proteoSUVs stock in 995 µL of dialysis 1× buffer A. Then add 5 µL of liposomes to the chamber containing 400 µL of buffer.

▲ **CRITICAL STEP** The dilution has to be adjusted to find a good compromise between the number of vesicles docked per hole. High dilution results in fewer vesicles per hole.

◆ **TROUBLESHOOTING**

22. Observe the same area under continuous illumination using medium laser intensity. Allow vesicles to dock on the membrane.
23. (Optional) Check that the green and red lasers are aligned correctly by imaging a multicolor fluorescent bead on a MaTeK glass-bottom dish. Ensure that the individual laser beams are imaged on the same area of the sample plane. Characteristics of vesicle docking are shown in Supplementary Video 2.
24. After the vesicles are docked on the membranes, the excess vesicles are removed with a new buffer.
25. Start the 'live' acquisition for 5,000 frames at 1,800 or 8,000 Hz (depending on the experimental requirement) to check the bilayer and vesicle dye fluorescence intensity imaging channels and the focus. The same protocol can be applicable for TIRF microscopy.
26. After starting live data acquisition for a small strip or area to monitor the fusion at a high temporal resolution, wait ~5 s and carefully introduce a drop of $CaCl_2$ solution (to reach a final 100 µM $CaCl_2$ concentration in the vesicle buffer) using a pipette.
27. Save movies of fields of view for both bilayer and vesicle channel channels. An example of vesicle fusion (lipid mixing) is shown in Supplementary Video 3.

Single-molecule imaging

● **TIMING ~2–3 h**

28. Start the 647 nm laser to observe Alexa 647 signals and/or open the shutter for the 488 nm laser to observe docked vesicle signals.
29. Drop immersion oil with a refractive index (n = 1.518) that matches that of the coverslip on a 60× NA 1.49 objective lens.

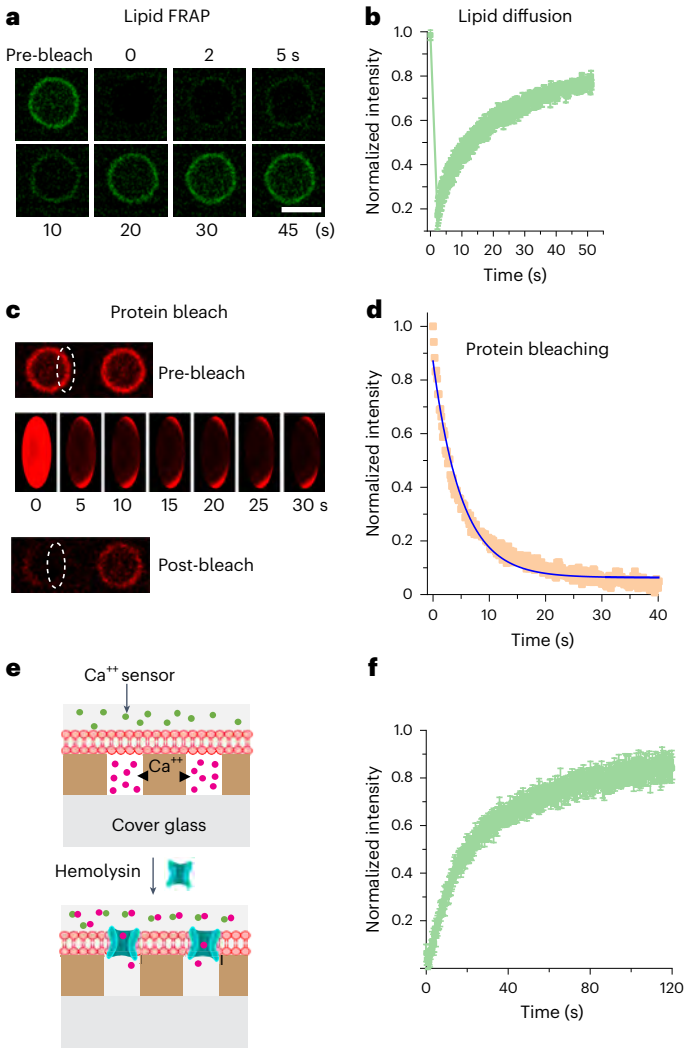

Fig. 6 | Bilayer characterization. a, An example of lipid FRAP showing rapid lipid fluorescence recovery after photo-bleaching. Scale bar, 5 µm. **b**, A representative lipid fluorescence recovery curve after bleaching. The lipid diffusion coefficient was calculated to be 2.4 $\mu m^2 s^{-1}$. **c**, An example of protein FRAP is shown. t-SNARE proteins were labeled with Alexa 647 NHS-ester. The dotted elliptical area was bleached continuously. As a result, all the proteins in that hole were bleached because of the protein diffusion. **d**, Protein fluorescence decay curve fitted with a single-exponential model. The protein diffusion coefficient was calculated to be 1.2 $\mu m^2 s^{-1}$. **e**, Unilamellarity of the suspended membrane was tested with alpha hemolysin. Initially, 25 mM Ca^{2+} (red sphere) was trapped under the suspended bilayer, and the calcium sensor, calcium green (green sphere) was added to the external buffer. Upon addition of hemolysin, Ca^{2+} ions diffused through pores and bound to calcium green, producing a rapid fluorescence increase. **f**, Fluorescence intensity trace of calcium green over time, confirming Ca^{2+} release through α-hemolysin pores and validating bilayer unilamellarity.

30. Place the samples on the stage of the TIRF microscope and adjust the lens position. Next, find a lipid bilayer area, and optimize the focus, intensity and incidence angle of the TIRF microscope excitation lasers.
31. Add the vesicles and Alexa Fluor 647-conjugated complexin.
32. Record live images using TIRF microscope by using the NIS-Elements software at a rate of 100 ms per frame.

Data analysis

● **TIMING ~10 h**

33. Run the ImageJ and/or MATLAB software to perform either step-wise bleaching analysis (option A) or vesicle docking and fusion analysis (option B).
    (A) **Stepwise bleaching-step analysis**
        (i) Load and visualize the image sequences in TIFF or JPEG format.
        (ii) Adjust the threshold to identify the vesicle puncta on the 488 nm channel images. Mark the region of interest (ROI) and apply the same ROI to the 647 nm channel.
        (iii) Using the plot *Z*-stack option to 'Track all frames' to measure the intensity at 488 and 647 nm channels.

(iv) Save the data in '.txt"' format and plot using any graphing software. If the step sizes are more than 5–7, the following methods were used to determine precise counts[43,44].

The photobleaching curves were fitted with an exponential decay curve with equation (1).

$$I(t) = I_0 e^{\frac{-t}{\tau}} + B \quad (1)$$

Where $I(t)$ denotes the intensity at time t, I_0 is the initial intensity before bleaching, τ is the time constant and B is the background. Hence, the copy number, N, can be obtained from equation (2).

$$N = \frac{I_0}{i} \quad (2)$$

where i is the average unit intensity of a single fluorophore as determined from the small clusters.

(B) **Vesicle-docking and fusion analysis**

(i) Perform vesicle docking and fusion analysis using ImageJ or MATLAB. Our previously published Fusion Analysis software and its source code are accessible on MATLAB Central[30]. Examples of vesicle docking under confocal and TIRF are shown in Supplementary Videos 2 and 4, respectively.

(ii) Use the dynamic puncta tracking algorithm to extract the information of vesicles in a space-time trajectory (x, y, t) and analyze lipid diffusion and cargo release fusion in a two-dimensional dataset. Centroid and Gaussian fit are used to track the location of the vesicles with high accuracy.

(iii) Use dynamic ROI coordinates of the fluorescent lipid of the vesicle channel to track the fluorescence of the content mixing channel at a given time.

Troubleshooting

Troubleshooting advice can be found in Table 1.

Table 1 | Troubleshooting table

Step	Problem	Possible reason	Solution
1A(v)	Not enough GPMVs	Not enough cells, vesiculation reagents (e.g., NEM) not functional, incubation time not enough	Try changing the concentration of NEM or using a different batch of the chemical. Try varying the treatment time and number of cells seeded. Minimize cell adherence to dish
1B(viii)	Not enough GUVs	Low concentration of lipids; not enough drying and rehydrating cycles	Increase the concentration of lipids. Repeated drying and hydration cycles can improve the yield and size of GUVs, probably from lipid reorganization in each cycle
21	Not enough vesicles docked	Low concentration of liposomes	Increase the number of liposomes added to the chamber

Timing

Step 1, GUV preparation: ~2–3 h
Steps 2–7, Cleaning chips: ~40 mins
Steps 8–14, Formation of lipid bilayer: ~2–3 h
Steps 15–19, Proteoliposomes preparation: 18–24 h
Steps 20–27, Vesicle preparation: 18–24 h
Steps 28–32, Single-moleculeimaging: ~2–3 h
Step 33, Data analysis: ~10 h

Anticipated results

Characterization of bilayer

Ensuring a continuous, fluid and unilamellar bilayer is essential for reproducible fusion assays. Representative FRAP data shown in Fig. 6a–d confirm that bilayers formed by bursting GUVs on pore arrays are laterally mobile, consistent with the properties of a fluid lipid bilayer. All bilayers were generated using synthetic lipids composed of 76.5% DOPC, 20% DOPS, 3% PIP_2 and 0.5% ATTO 465-DOPE. To verify bilayer unilamellarity and transmembrane barrier function, we used α-hemolysin to form pores in the suspended membranes. Before pore insertion, Ca^{2+}-sensitive fluorophores were present on one side of the bilayer, while Ca^{2+} ions were restricted to the opposite side, resulting in no fluorescence signal. Upon α-hemolysin incorporation, pore formation allows Ca^{2+} ions to diffuse across the membrane and bind to the fluorophores, leading to a measurable fluorescence increase (Fig. 6d,e). This confirms that the bilayer effectively separates the two compartments and permits selective molecular exchange only through defined transmembrane pores.

Vesicle docking and fusion analysis

When this assay is performed successfully, users can expect to observe real-time docking and fusion of SRB-loaded vesicles on suspended planar membranes with high temporal precision. Before calcium addition, vesicles reconstituted with VAMP2 and SYT1 stably dock onto the bilayer containing preassembled t-SNAREs. These events appear as immobile fluorescent spots, and their arrival is marked by a rapid increase in signal followed by a steady plateau (Fig. 7a). Multiple docking traces typically show stable fluorescence intensity over time, indicating vesicle immobilization without spontaneous fusion. Representative examples are shown in Supplementary Videos 2 and 4, acquired using confocal and TIRF microscopy, respectively.

Occasionally, vesicles may undergo spontaneous fusion before calcium stimulation. These vesicles remain mobile on the membrane surface until they fuse, which is reflected by a sudden fluorescence increase due to SRB dequenching (Fig. 7b). Although rare, such events highlight the stochastic nature of membrane fusion under resting conditions.

Upon addition of 100 μM Ca^{2+}, synchronized fusion events are commonly observed. Time-lapse imaging reveals vesicles fusing within milliseconds of calcium exposure, with no noticeable diffusion preceding fusion. Two representative vesicles display simultaneous signal increases in the content channel, consistent with Ca^{2+}-triggered fusion (Fig. 7c). Intensity profiles of these vesicles (Fig. 7d) show sharp rises corresponding to fusion, followed by stable plateaus and gradual photobleaching. Post-Ca^{2+} addition, statistically significant intensity jumps occur at variable timepoints depending on experimental conditions such as Ca^{2+} concentration, lipid composition, and membrane curvature. A ≥2-fold increase in content-mixing fluorescence is typically considered a fusion event. Higher Ca^{2+} concentrations (>100 μM) generally yield faster and more pronounced fluorescence increases. To ensure statistically robust conclusions, analysis of at least 500–1,000 fusion events is recommended, with ≥5,000 events providing high-precision kinetic measurements. Supplementary Videos 3 and 5 show representative results for lipid mixing (confocal) and content mixing (TIRF), respectively. Analyzing hundreds to thousands of time traces enables the generation of statistically meaningful histograms and accurate mechanistic insights into fusion kinetics. The synchronized calcium-triggered fusion described here is mediated by SNAREs and SYT1 in the presence of complexin. Notably, complexin significantly enhances synchronous fusion at 100 μM Ca^{2+}. Ongoing work is exploring the contributions of additional regulatory proteins in this system, including Munc18 and Munc13.

Across large datasets, users should expect diverse fusion kinetics. Some vesicles fuse immediately after calcium addition, others with delays, and a few may fuse without showing a clear SRB dequenching signal, probably due to insufficient dye loading or incomplete quenching (Fig. 7e). These trace types, synchronous or delayed, are expected in a typical dataset and reflect the heterogeneity of vesicle populations.

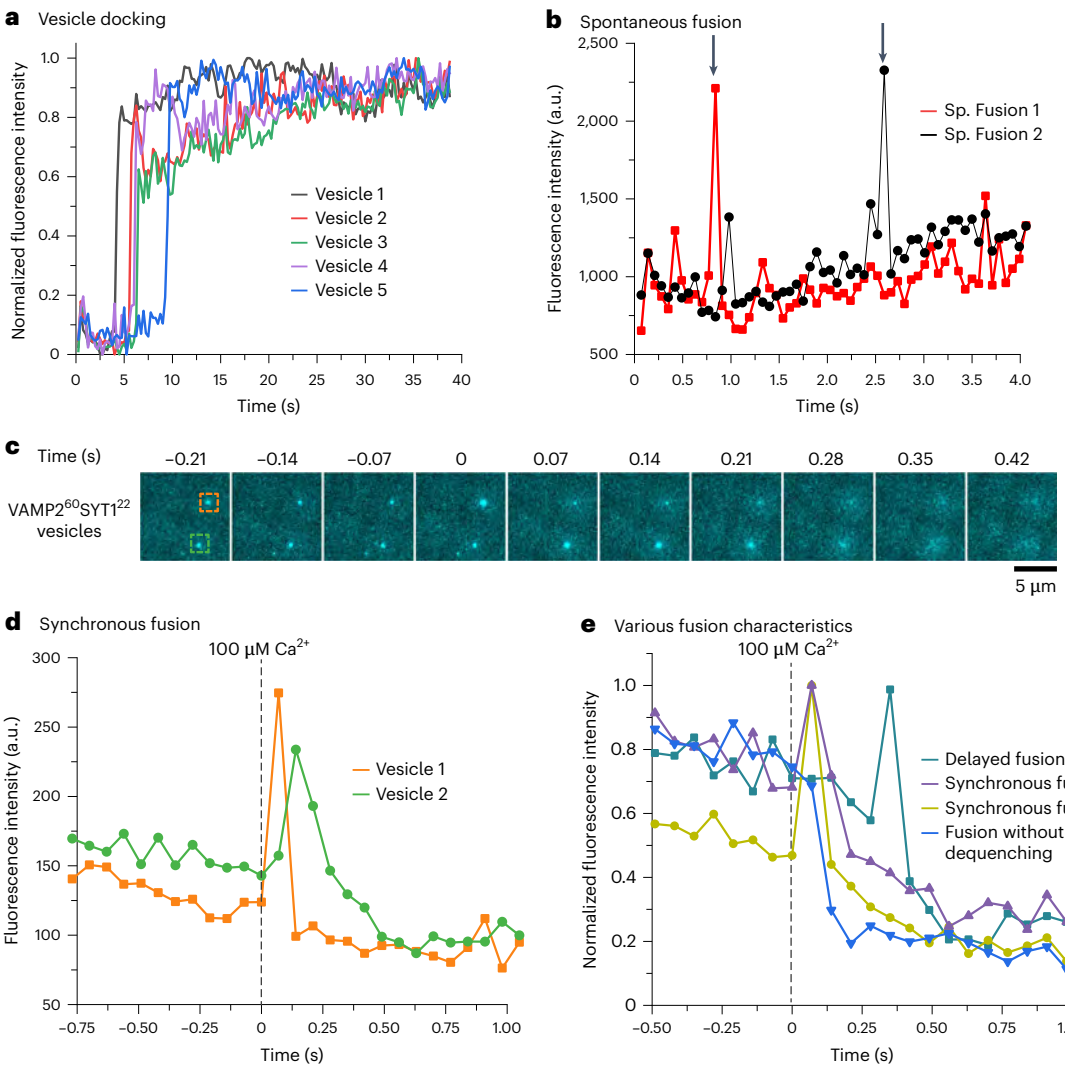

Fig. 7 | Dynamic monitoring of vesicle docking and fusion. Docking and fusion profiles of SRB-loaded, VAMP2^{60}SYT1^{22} vesicles. **a**, Vesicles first appear on the membrane containing pre-assembled t-SNAREs and quickly dock (immobile) on the membrane. ROIs (6 × 6 pixel) were drawn around the respective immobile vesicle. A rapid jump in intensity denotes the arrival of the vesicle and vesicles remain immobile at the same spots for a long time. Five separate examples are shown here. A representative vesicle docking is shown in Supplementary Video 4. **b**, Two representative spontaneous (sp.) fusion traces are shown. Vesicles continuously diffuse on the membrane before undergoing spontaneous fusion. ROIs were drawn around the fusion spots. A rapid increase in signal dictates SRB dequenching as a result of spontaneous fusion. **c**, A time-lapse series of images of SRB-loaded VAMP2^{60}SYT1^{22} vesicles. 100 µM Ca^{2+} was added at time 0. Two vesicles (marked in dotted orange and green boxes) fused synchronously upon arrival of Ca^{2+}. The images were captured every 70 ms. Scale bar, 5 µm. **d**, Intensity profiles of the two vesicles are plotted. Orange and green lines represent the corresponding vesicles shown in **c**. **e**, Various types of fusion traces are shown. Two vesicles (magenta and yellow) fused synchronously whereas green represents delayed fusion. The blue trace represents a fusion profile without noticeable SRB dequenching which suggests that this vesicle does not contain enough SRB to be in a quenched state.

Single-molecule counting

Single-molecule counting data were collected by measuring AlexaFluor 647-labeled complexin fluorescence intensity over time. Each trace was plotted as a function of time using ImageJ and bleaching steps were counted (Fig. 8). The protocol presented here is to measure the number of complexin molecules. However, the methodology can be extended to counting any labeled protein of interest.

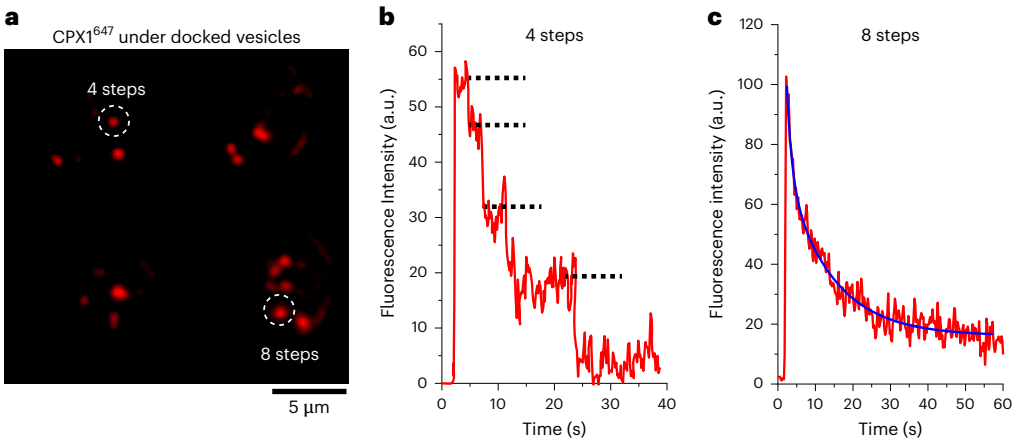

Fig. 8 | Single-molecule counting by photobleaching in suspended lipid bilayers. a, The fluorescence microscopy images of Alexa-647 conjugated complexin 1 protein under docked vesicles, two highlighted examples with '4 steps' and '8 steps' photobleaching events indicated by dashed circles. Scale bar, 5 µm. **b**,**c**, The corresponding fluorescence intensity decay graphs for the '4 steps' (**b**) and '8 steps' (**c**) events, as detected in single-molecule photobleaching, with the *y* axis representing fluorescence intensity.

Data availability

The vesicle fusion data generated during this study and source data files detailing the underlying processed dataset are provided. Source data are provided with this paper.

Code availability

The 'Fusion Analyzer' package is available on GitHub (https://github.com/sathishramakrishnan/fas) and MATLAB central (https://www.mathworks.com/matlabcentral/fileexchange/66521-fusion-analyzer-fas).

Received: 11 January 2024; Accepted: 4 April 2025;
Published online: 03 June 2025

References

1. Rothman, J. E. The principle of membrane fusion in the cell (Nobel Lecture. *Angew. Chem. Int. Edit.* **53**, 12676–12694 (2014).
2. Trimbuch, T. & Rosenmund, C. Should I stop or should I go? The role of complexin in neurotransmitter release. *Nat. Rev. Neurosci.* **17**, 118–125 (2016).
3. Kaeser, P. S. & Regehr, W. G. Molecular mechanisms for synchronous, asynchronous, and spontaneous neurotransmitter release. *Annu. Rev. Physiol.* **76**, 333–363 (2014).
4. Brunger, A. T., Choi, U. B., Lai, Y., Leitz, J. & Zhou, Q. Molecular mechanisms of fast neurotransmitter release. *Annu. Rev. Biophys.* **47**, 469–497 (2018).
5. Rizo, J. Molecular mechanisms underlying neurotransmitter release. *Annu. Rev. Biophys.* **51**, 377–408 (2022).
6. Sudhof, T. C. Neurotransmitter release: the last millisecond in the life of a synaptic vesicle. *Neuron* **80**, 675–690 (2013).
7. Boyken, J. et al. Molecular profiling of synaptic vesicle docking sites reveals novel proteins but few differences between glutamatergic and GABAergic synapses. *Neuron* **78**, 285–297 (2013).
8. Weingarten, J. et al. The proteome of the presynaptic active zone from mouse brain. *Mol. Cell. Neurosci.* **59**, 106–118 (2014).
9. Holderith, N., Heredi, J., Kis, V. & Nusser, Z. A high-resolution method for quantitative molecular analysis of functionally characterized individual synapses. *Cell Rep.* **32**, 107968 (2020).
10. Gallagher, B. R. & Zhao, Y. X. Expansion microscopy: a powerful nanoscale imaging tool for neuroscientists. *Neurobiol. Dis.* **154**, 105362 (2021).
11. Kyoung, M. et al. In vitro system capable of differentiating fast Ca_2^+-triggered content mixing from lipid exchange for mechanistic studies of neurotransmitter release. *Proc. Natl Acad. Sci. USA* **108**, E304–E313 (2011).
12. Diao, J., Zhao, M., Zhang, Y., Kyoung, M. & Brunger, A. T. Studying protein-reconstituted proteoliposome fusion with content indicators in vitro. *Bioessays* **35**, 658–665 (2013).
13. Kyoung, M., Zhang, Y., Diao, J., Chu, S. & Brunger, A. T. Studying calcium-triggered vesicle fusion in a single vesicle-vesicle content and lipid-mixing system. *Nat. Protoc.* **8**, 1–16 (2013).
14. Leitz, J. et al. Observing isolated synaptic vesicle association and fusion ex vivo. *Nat. Protoc.* https://doi.org/10.1038/s41596-024-01014-x (2024).
15. Tucker, W. C., Weber, T. & Chapman, E. R. Reconstitution of Ca_2^+-regulated membrane fusion by synaptotagmin and SNAREs. *Science* **304**, 435–438 (2004).
16. Gong, B. et al. High affinity host–guest FRET pair for single-vesicle content-mixing assay: observation of flickering fusion events. *J. Am. Chem. Soc.* **137**, 8908–8911 (2015).
17. Lee, H.-K. et al. Dynamic Ca_2^+-dependent stimulation of vesicle fusion by membrane-anchored synaptotagmin 1. *Science* **328**, 760–763 (2010).
18. Pantazatos, D. & MacDonald, R. Directly observed membrane fusion between oppositely charged phospholipid bilayers. *J. Membr. Biol.* **170**, 27–38 (1999).
19. Witkowska, A. & Jahn, R. Rapid SNARE-mediated fusion of liposomes and chromaffin granules with giant unilamellar vesicles. *Biophys. J.* **113**, 1251–1259 (2017).
20. Tareste, D., Shen, J., Melia, T. J. & Rothman, J. E. SNAREpin/Munc18 promotes adhesion and fusion of large vesicles to giant membranes. *Proc. Natl Acad. Sci. USA* **105**, 2380–2385 (2008).

21. Kiessling, V., Domanska, M. K. & Tamm, L. K. Single SNARE-mediated vesicle fusion observed in vitro by polarized TIRFM. *Biophys. J.* **99**, 4047–4055 (2010).
22. Domanska, M. K., Kiessling, V., Stein, A., Fasshauer, D. & Tamm, L. K. Single vesicle millisecond fusion kinetics reveals number of SNARE complexes optimal for fast SNARE-mediated membrane fusion. *J. Biol. Chem.* **284**, 32158–32166 (2009).
23. Karatekin, E. et al. A fast, single-vesicle fusion assay mimics physiological SNARE requirements. *Biophys. J.* **98**, 616a (2010).
24. Bao, H. et al. Dynamics and number of trans-SNARE complexes determine nascent fusion pore properties. *Nature* **554**, 260–263 (2018).
25. Bera, M., Ramakrishnan, S., Coleman, J., Krishnakumar, S. S. & Rothman, J. E. Molecular determinants of complexin clamping and activation function. *eLife* **11**, e71938 (2022).
26. Ramakrishnan, S., Bera, M., Coleman, J., Rothman, J. E. & Krishnakumar, S. S. Synergistic roles of synaptotagmin-1 and complexin in calcium-regulated neuronal exocytosis. *eLLife* **9**, e54506 (2020).
27. Ramakrishnan, S. et al. Synaptotagmin oligomers are necessary and can be sufficient to form a Ca_2^+-sensitive fusion clamp. *FEBS Lett.* **593**, 154–162 (2019).
28. Coleman, J. et al. PRRT2 regulates synaptic fusion by directly modulating SNARE complex assembly. *Cell Rep.* **22**, 820–831 (2018).
29. Heo, P. et al. Highly reproducible physiological asymmetric membrane with freely diffusing embedded proteins in a 3D-printed microfluidic setup. *Small* **15**, e1900725 (2019).
30. Ramakrishnan, S. et al. High-throughput monitoring of single vesicle fusion using freestanding membranes and automated analysis. *Langmuir* **34**, 5849–5859 (2018).
31. Schwenen, L. L. et al. Resolving single membrane fusion events on planar pore-spanning membranes. *Sci. Rep.* **5**, 12006 (2015).
32. Mühlenbrock, P., Herwig, K., Vuong, L., Mey, I. & Steinem, C. Fusion pore formation observed during SNARE-mediated vesicle fusion with pore-spanning membranes. *Biophys. J.* **119**, 151–161 (2020).
33. Hubrich, R., Park, Y., Mey, I., Jahn, R. & Steinem, C. SNARE-mediated fusion of single chromaffin granules with pore-spanning membranes. *Biophys. J.* **116**, 308–318 (2019).
34. Kalyana Sundaram, R. V. et al. Native planar asymmetric suspended membrane for single-molecule investigations: plasma membrane on a chip. *Small* **18**, 2205567 (2022).
35. Krishnakumar, S. S. et al. Conformational dynamics of calcium-triggered activation of fusion by synaptotagmin. *Biophys. J.* **105**, 2507–2516 (2013).
36. Takamori, S. et al. Molecular anatomy of a trafficking organelle. *Cell* **127**, 831–846 (2006).
37. Weber, T. et al. SNAREpins: minimal machinery for membrane fusion. *Cell* **92**, 759–772 (1998).
38. Shi, L. et al. SNARE proteins: one to fuse and three to keep the nascent fusion pore open. *Science* **335**, 1355–1359 (2012).
39. Shen, J., Tareste, D. C., Paumet, F., Rothman, J. E. & Melia, T. J. Selective activation of cognate SNAREpins by Sec1/Munc18 proteins. *Cell* **128**, 183–195 (2007).
40. Giraudo, C. G., Eng, W. S., Melia, T. J. & Rothman, J. E. A clamping mechanism involved in SNARE-dependent exocytosis. *Science* **313**, 676–680 (2006).
41. Kummel, D. et al. Complexin cross-links prefusion SNAREs into a zigzag array. *Nat. Struct. Mol. Biol.* **18**, 927–933 (2011).
42. Ji, H. et al. Protein determinants of SNARE-mediated lipid mixing. *Biophys. J.* **99**, 553–560 (2010).
43. Bera, M. et al. Synaptophysin chaperones the assembly of 12 SNAREpins under each ready-release vesicle. *Proc. Natl Acad. Sci.* **120**, e2311484120 (2023).
44. Li, F. et al. Vesicle capture by membrane-bound Munc13-1 requires self-assembly into discrete clusters. *FEBS Lett.* **595**, 2185–2196 (2021).

Acknowledgements

This study was supported by grants to S.R. from Yale Pathology, the Yale Diabetes Center (P30 DK045735) and the Yale Alzheimer's Disease Research Center. S.R. would like to thank J. Pichurin and J.E. Rothman, for their proofreading and critical insights into the protocol.

Author contributions

M.B., R.V.K.S. and S.R. performed the experiments. M.B., R.V.K.S., A.C. and S.R. wrote the manuscript and made the figures. S.R. conceived the idea of the SLIM platform, designed and developed it with F.P. S.T. and J.C. maintained cells and provided proteins.

Competing interests

The authors declare no competing interests.

Additional information

Supplementary information The online version contains supplementary material available at https://doi.org/10.1038/s41596-025-01192-2.

Correspondence and requests for materials should be addressed to Frederic Pincet or Sathish Ramakrishnan.

Peer review information *Nature Protocols* thanks Yang Yang, Jiajie Diao and the other, anonymous, reviewer(s) for their contribution to the peer review of this work.